Figure S1

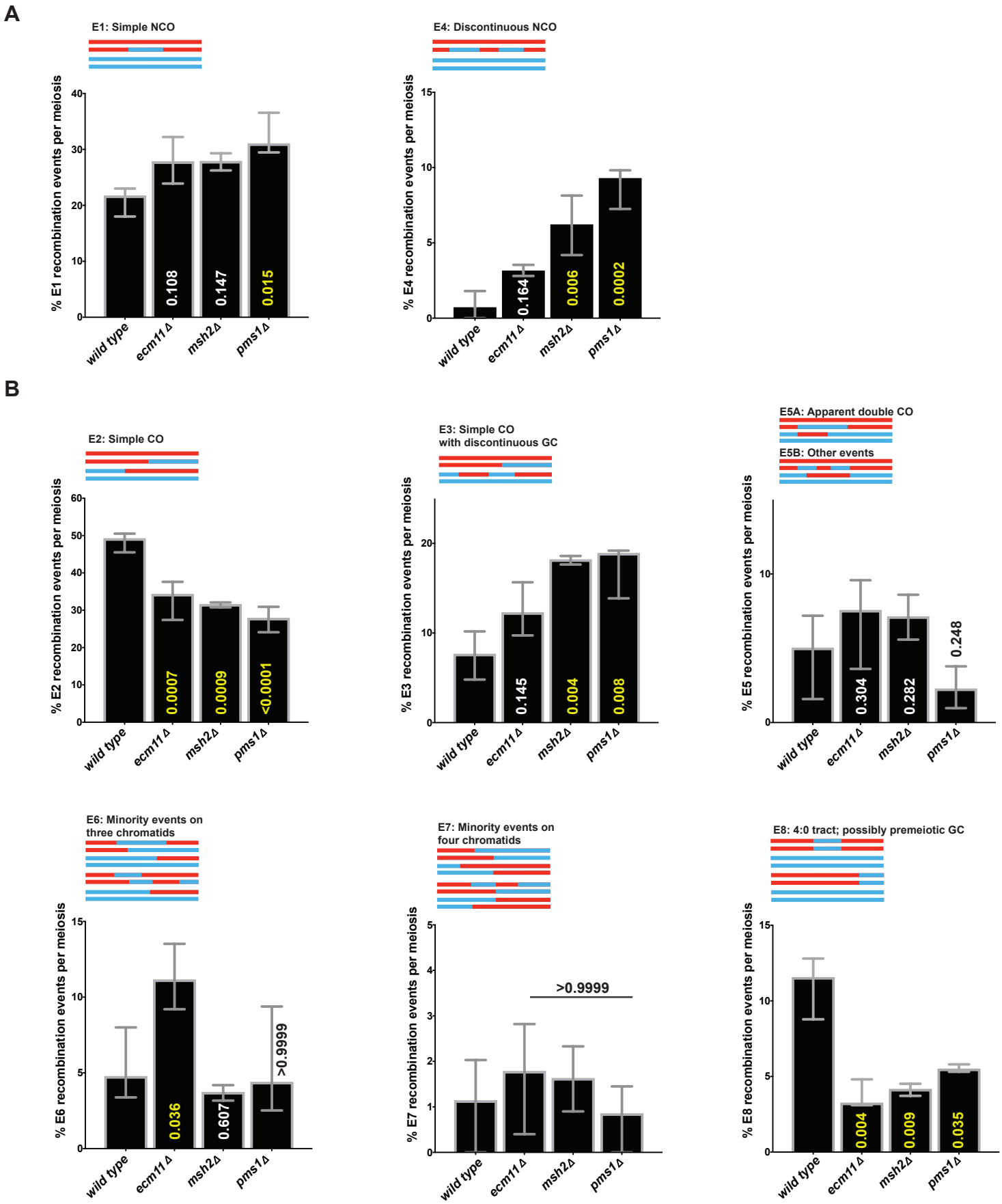
A
E1: Simple NCO
% E1 recombination events per meiosis
0.108
0.147
0.015
wild type
ecm11Δ
msh2Δ
pms1Δ
E4: Discontinuous NCO
% E4 recombination events per meiosis
0.164
0.006
0.0002
B
E2: Simple CO
% E2 recombination events per meiosis
0.0007
0.0009
<0.0001
E3: Simple CO
with discontinuous GC
% E3 recombination events per meiosis
0.145
0.004
0.008
E5A: Apparent double CO
E5B: Other events
% E5 recombination events per meiosis
0.304
0.282
0.248
E6: Minority events on
three chromatids
% E6 recombination events per meiosis
0.036
0.607
>0.9999
E7: Minority events on
four chromatids
% E7 recombination events per meiosis
>0.9999
E8: 4:0 tract; possibly premeiotic GC
% E8 recombination events per meiosis
0.004
0.009
0.035

Figure S1. Genome-wide sequence analysis of *ecm11* meiotic products indicates a role for SC central element in limiting both majority and minority interhomolog recombination events.
(Relates to Figure 2)
Bar graphs indicate the proportion of specific interhomolog recombination events found in four wild type, five *ecm11*, two *msh2*, and three *pms1* Octad Rec-Seq datasets; median and range values for each strain are plotted. *P* values obtained by Fisher's Exact test (indicated in yellow if significant, white if not significant) indicate whether the average proportion of a particular class of recombination events in each mutant is significantly different from the average proportion found in wild type. Recombination event categories are described in Methods, and data plotted in these graphs is listed in Table 2. Note chromosome 7 recombination events were excluded for all octads, due to chromosome 7 disomy in two wild-type samples.

Figure S2

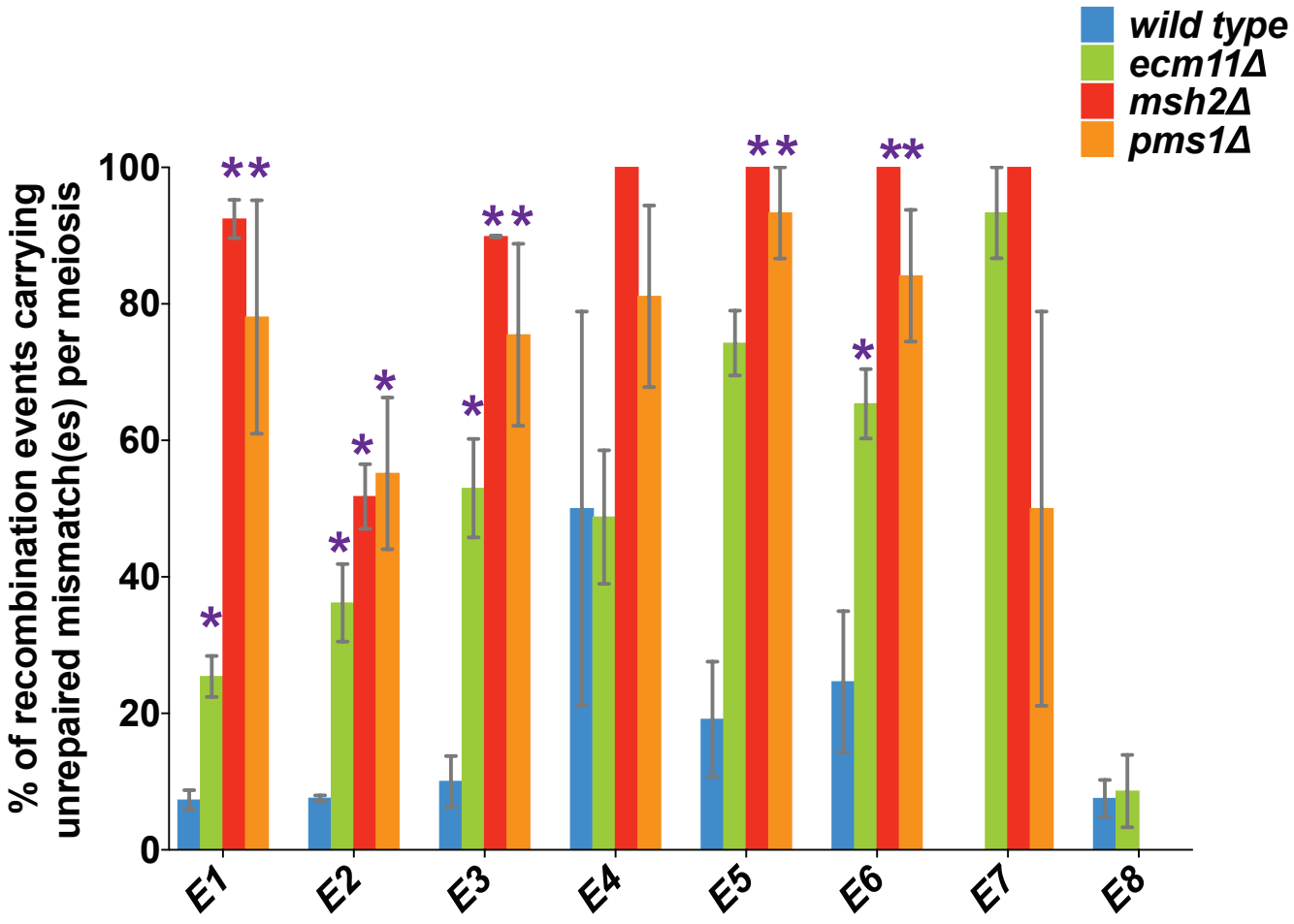
wild type
ecm11Δ
msh2Δ
pms1Δ
% of recombination events carrying unrepaired mismatch(es) per meiosis
100
80
60
40
20
0
E1
E2
E3
E4
E5
E6
E7
E8
*
**

Figure S2. *ecm11* mutants exhibit an increased number of unrepaired mismatch-carrying events in several categories of recombination.

(Relates to Figure 3)

Column graph plots the median and range percentage of specific classes of recombination events (indicated on the *x* axis) that display unrepaired mismatches in four wild-type (blue), five *ecm11* (green), two *msh2* (red), and three *pms1* (orange) octads. For each class of recombination event, strains showing significant differences relative to wild type are labeled with a purple asterisk (two-tailed *P* values obtained using a Fisher's Exact test). The proportion of E1 recombination events with unrepaired mismatches for *ecm11*, *msh2,* and *pms1* are significantly increased relative to wild type (P=0.045 <0.0001, <0.0001 respectively). The proportion of E2 and E3 recombination events with unrepaired mismatches is also significantly increased in *ecm11*, *msh2,* and *pms1* (P <0.0001 for E2 in each strain; P= 0.04, <0.0001, 0.0007 respectively, for E3). The proportion of E5 recombination events with unrepaired mismatches is not significantly different between wild-type and *ecm11* (P=0.69), but is significantly different between wild-type and *msh2,* or *pms1* (P=0.0006, and 0.028 respectively). Finally, the proportion of E6 recombination events with unrepaired mismatches is significantly different from wild-type in *ecm11*, *msh2*, and *pms1* (P=0.045, 0.007, 0.019, respectively). Note chromosome 7 recombination events for two wild-type octads were excluded from the analysis due to chromosome 7 disomy.

Figure S3

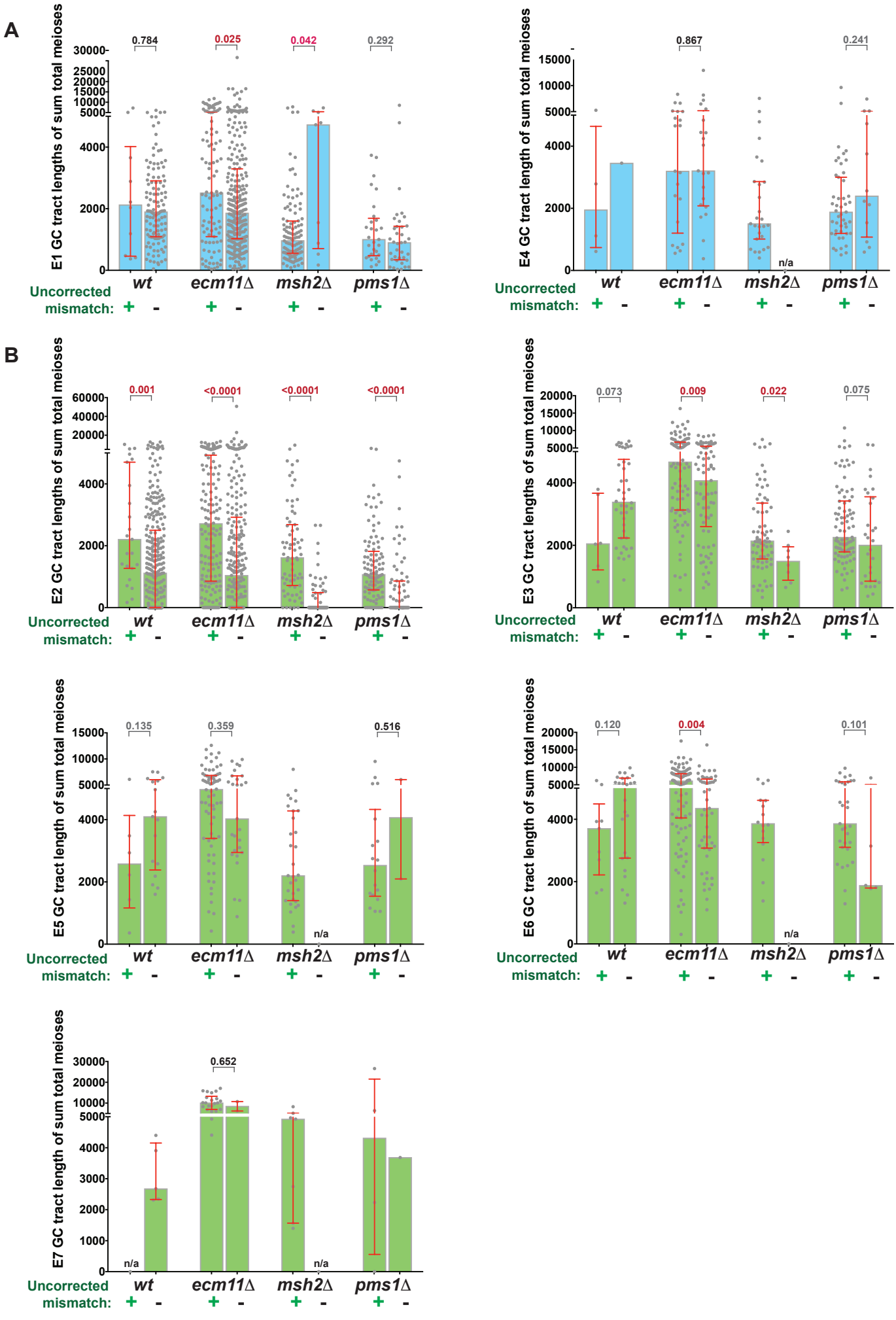
A
E1 GC tract lengths of sum total meioses
0.784
0.025
0.042
0.292
E4 GC tract length of sum total meioses
0.867
0.241
n/a
B
E2 GC tract lengths of sum total meioses
0.001
<0.0001
<0.0001
<0.0001
E3 GC tract lengths of sum total meioses
0.073
0.009
0.022
0.075
E5 GC tract length of sum total meioses
0.135
0.359
0.516
n/a
E6 GC tract length of sum total meioses
0.120
0.004
0.101
n/a
E7 GC tract length of sum total meioses
0.652
n/a
n/a
Uncorrected mismatch:
+ -
wt
ecm11Δ
msh2Δ
pms1Δ

Figure S3. Gene conversion tracts with unrepaired mismatches often average longer than their mismatch-free counterparts in *ecm11* mutants.

(Relates to Figure 4)

Each circle on the scatterplots represents a gene conversion tract length (# nucleotides) associated with a noncrossover (light blue shading, **A**) or crossover (green shading, **B**) class of recombination events. Total gene conversion tract lengths with each type of recombination signature (E1-E7) from four wild-type, five *ecm11*, two *msh2*, and four *pms1* meioses (Octad Rec-Seq datasets) are plotted in separate columns depending on whether the event carries an unrepaired mismatch (indicated below with a + or -; strains listed on the *x* axis). Height of the shaded area indicates a median value for each group, while red error bars indicate interquartile range. Two-tailed *P* values using a Mann-Whitney test are indicated above the error bars (red if significant). Note chromosome 7 recombination events for two wild-type octads were excluded from these analyses, due to chromosome 7 disomy.

Figure S4

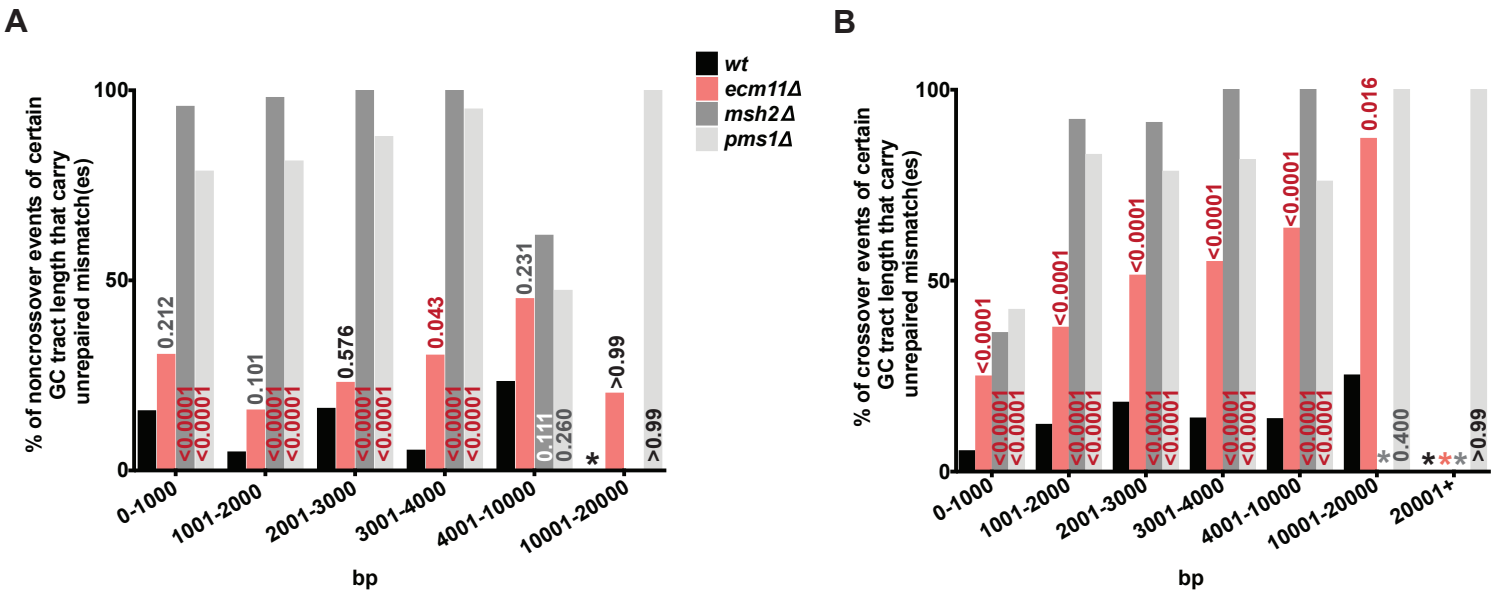
A
B
wt
ecm11Δ
msh2Δ
pms1Δ
% of noncrossover events of certain GC tract length that carry unrepaired mismatch(es)
% of crossover events of certain GC tract length that carry unrepaired mismatch(es)
100
50
0
0.212
<0.0001
<0.0001
0.101
<0.0001
<0.0001
0.576
<0.0001
<0.0001
0.043
<0.0001
<0.0001
0.231
0.111
0.260
*
>0.99
>0.99
<0.0001
<0.0001
<0.0001
<0.0001
<0.0001
<0.0001
<0.0001
<0.0001
<0.0001
<0.0001
<0.0001
<0.0001
<0.0001
<0.0001
<0.0001
0.016
*
0.400
*
*
*
>0.99
0-1000
1001-2000
2001-3000
3001-4000
4001-10000
10001-20000
20001+
bp

Figure S4. Elevated frequency of unrepaired mismatches in *ecm11* mutants regardless of gene conversion tract length.

(Relates to Figure 5, Table S2)

Column graphs plot the percentage of unrepaired mismatch-carrying noncrossover (**A**) or crossover (**B**) events with gene conversion tracts of distinct length ranges (indicated on the *x* axis). Data plotted is consolidated from all genome-wide recombination events identified in four wild-type (black bars), five *ecm11* (pink bars), two *msh2* (gray bars) and three *pms1* (silver bars) meioses (Octad Rec-Seq datasets). For each category of tract length, a Fisher's Exact test was used to determine whether the proportion of unrepaired mismatch-carrying recombination events is significantly different in any of the mutant strains relative to wild-type (*P* values are indicated on the graph; red indicates statistical significance). The proportion of noncrossovers carrying an unrepaired mismatch in *ecm11* is only significantly greater than wild-type in the 3001-4000 tract length category, but the proportion of crossovers carrying an unrepaired mismatch in *ecm11* is significantly greater than wild-type for every tract length category. The raw data plotted in (**A**, **B**) is given in Table S2. Note chromosome 7 recombination events for two wild-type octads were excluded from these analyses, due to chromosome 7 disomy.

Figure S5

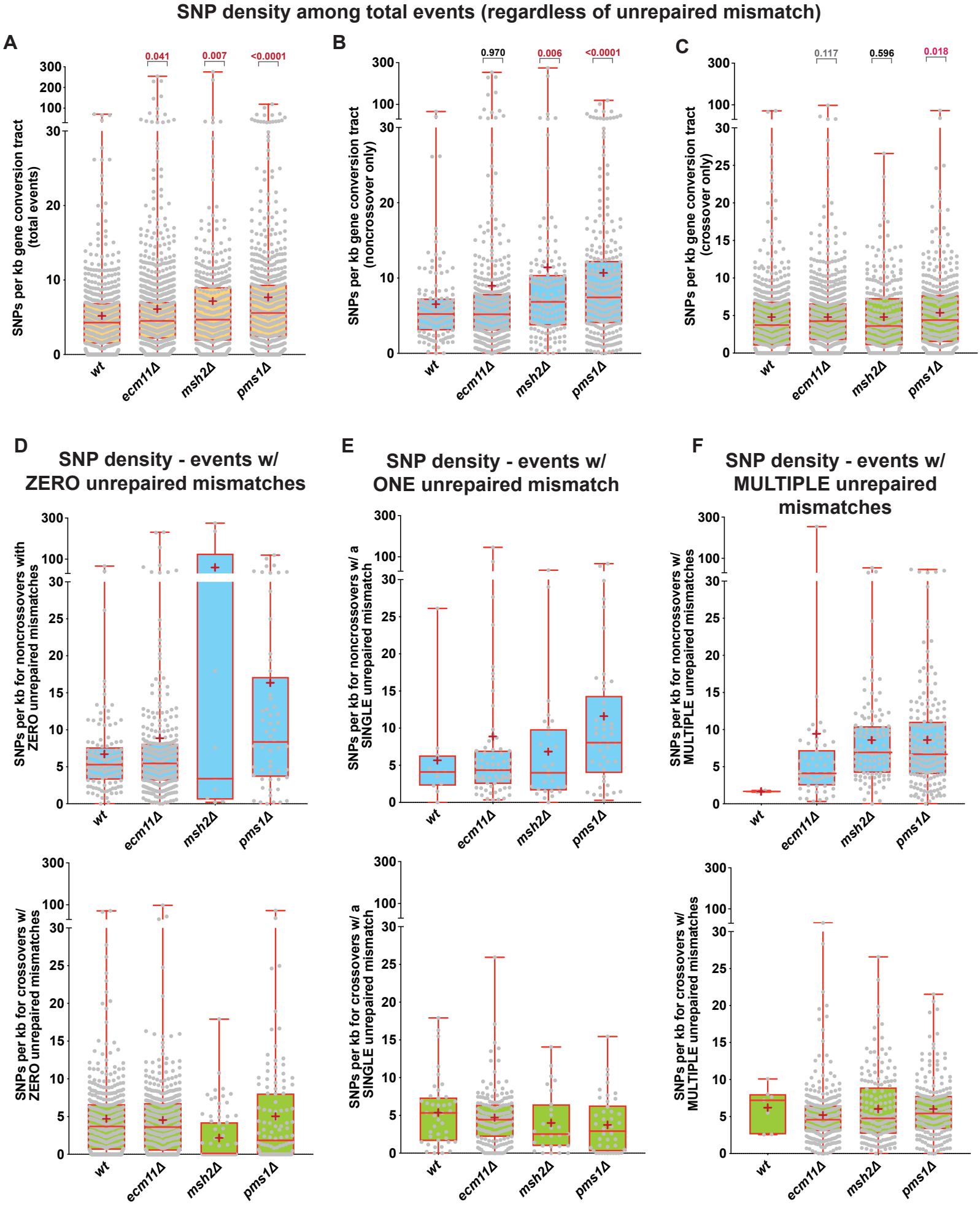
SNP density among total events (regardless of unrepaired mismatch)
A
SNPs per kb gene conversion tract (total events)
0.041
0.007
<0.0001
B
SNPs per kb gene conversion tract (noncrossover only)
0.970
0.006
<0.0001
C
SNPs per kb gene conversion tract (crossover only)
0.117
0.596
0.018
wt
ecm11Δ
msh2Δ
pms1Δ
D
SNP density - events w/ ZERO unrepaired mismatches
SNPs per kb for noncrossovers with ZERO unrepaired mismatches
SNPs per kb for crossovers w/ ZERO unrepaired mismatches
E
SNP density - events w/ ONE unrepaired mismatch
SNPs per kb for noncrossovers w/ a SINGLE unrepaired mismatch
SNPs per kb for crossovers w/ a SINGLE unrepaired mismatch
F
SNP density - events w/ MULTIPLE unrepaired mismatches
SNPs per kb for noncrossovers w/ MULTIPLE unrepaired mismatches
SNPs per kb for crossovers w/ MULTIPLE unrepaired mismatches

Figure S5. SNP density in *ecm11* gene conversion tracts is similar to wild type.
Grey circles in each box whisker plot represents a single nucleotide polymorphism (SNP) density measurement (SNP per kilobase) for individual gene conversion tracts in four wild-type, five *ecm11*, two *msh2* and three *pms1* meioses. The shaded box encompasses the 25th to 75th percentile (middle 50%) of values, red bar within the shaded area indicates the median, red vertical bars indicate the range, and red + indicates the mean for each genotype. Graphs in (**A**-**C**) plot SNP density values for total interhomolog recombination events regardless of the presence of an unrepaired mismatch (**A**, yellow shading), for all noncrossover (E1 + E4) events regardless of an unrepaired mismatch (**B**, blue shading), and for all crossover (E2, E3, E5, E6, E7) events regardless of an unrepaired mismatch (**C**, green shading). *P* values to described statistical differences between mutant and wild type SNP densities, calculated using the Mann Whitney test. are indicated above mutant columns; see Results narrative for additional *P* values calculated after particular high SNP density outliers are removed (relevant for the total *ecm11* and *msh2* noncrossover tract comparisons). Graphs in (**D**-**F**) plot SNP density values of noncrossover (blue shading, upper) or crossover (green shading, lower) events that display zero (**D**), one (**E**), or more than one (**F**) unrepaired mismatch. For *ecm11*, the population of tracts with a single unrepaired mismatch do not show a strongly significant increase in SNP density relative to the population of tracts with zero unrepaired mismatches (*P* calculated using the Mann Whitney test = 0.05 for crossovers, $P = 0.07$ for noncrossovers), and the population of tracts with multiple unrepaired mismatches do not show a strongly significant increase in SNP density relative to the population of tracts with a single unrepaired mismatch ($P = 0.15$ for crossovers, $P = 0.96$ for noncrossovers). Note chromosome 7 recombination events for two wild-type octads were excluded from these analyses, due to chromosome 7 disomy.

Figure S6

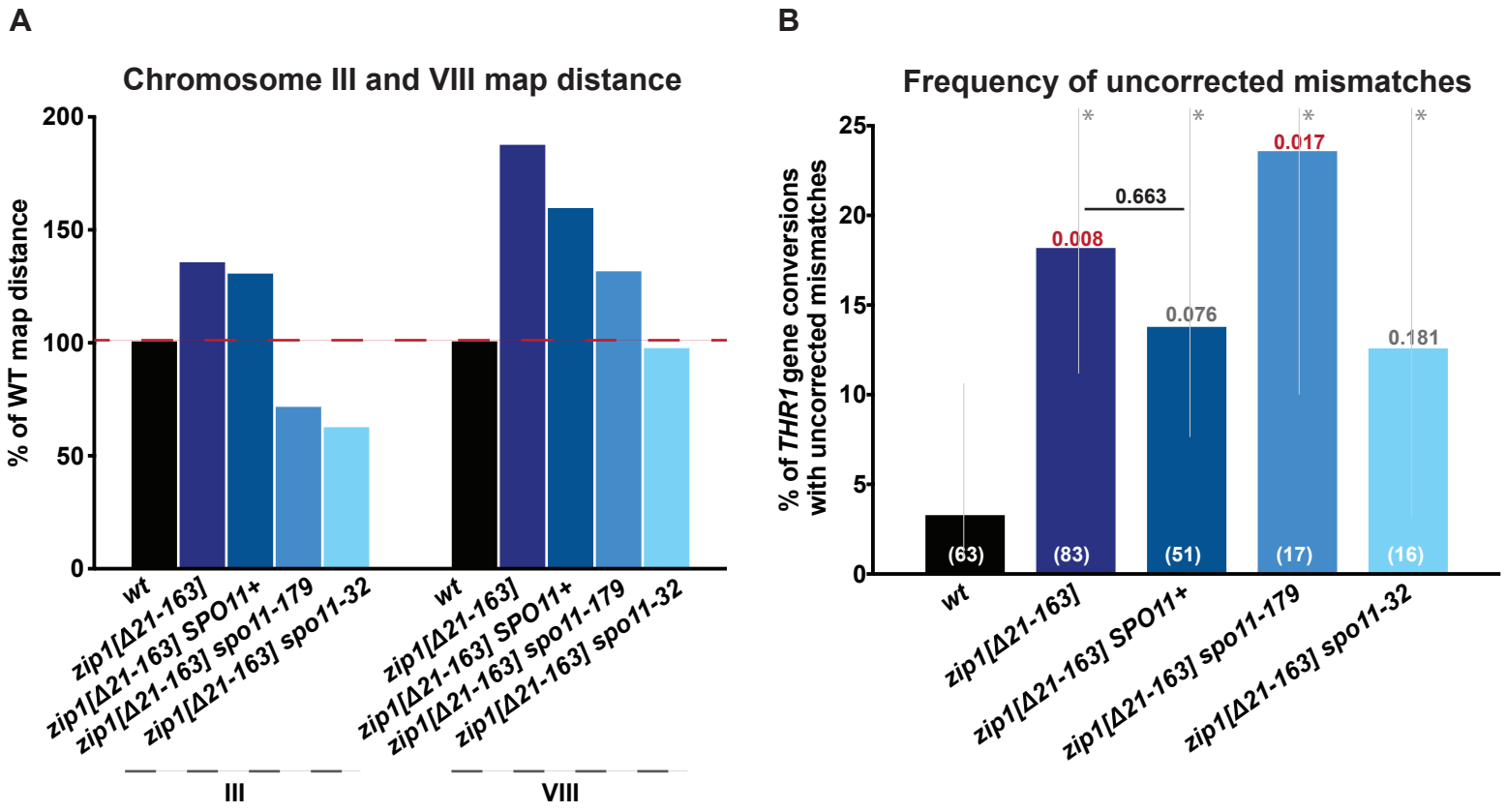
A
Chromosome III and VIII map distance
% of WT map distance
200
150
100
50
0
wt
zip1[Δ21-163]
zip1[Δ21-163] SPO11+
zip1[Δ21-163] spo11-179
zip1[Δ21-163] spo11-32
III
VIII
B
Frequency of uncorrected mismatches
% of THR1 gene conversions with uncorrected mismatches
25
20
15
10
5
0
0.008
0.663
0.076
0.017
0.181
(63)
(83)
(51)
(17)
(16)
*

Figure S6. The mismatch repair defect apparent in SC-deficient mutants is not likely due to saturation of mismatch repair machinery caused by elevated DNA double strand breaks.
Graph in (**A**) plots the genetic map length of chromosome III (left cluster) and chromosome VIII (right cluster), in *zip1[Δ21-163]* diploids homozygous for either *SPO11+* (navy bar) or two different *spo11* hypomorphic alleles (light blue bars). Five genetic markers spanning chromosome III and four genetic markers, including *THR1/thr1-4*, along the length of chromosome VIII were used to calculate map distances (See Table S1 for full genetic map data). Summed genetic map distances between all intervals on III and VIII are displayed as a percentage of the wild-type value. A reduction in the genetic map length relative to both *zip1[Δ21-163] SPO11+* and wild type is observed in each strain carrying a *spo11* hypomorphic allele. Graph in (**B**) plots the percentage of *THR1* gene conversion-associated tetrads with a phenotypically sectored colony on SC-Thr (a non-conventional gene conversion event (post-meiotic segregation) reflecting an unrepaired mismatch at the *THR1* locus), for each of the *zip1[Δ21-163]* strains homozygous for *spo11* reduction-of-function alleles as well as the control (*SPO11+*) strain. The total number of tetrads (meioses) observed with nonmendelian segregation (conventional or non-conventional) at *THR1* is indicated (in white) at the bottom of the corresponding bar for each strain. A two-tailed *P* value for each set of mutant data compared with wild type, calculated using a Fisher's Exact test, is indicated above individual columns (values in red are considered statistically significant, grey not quite significant, and black not significant). All three CRISPR-Cas9 manipulated *zip1[Δ21-163]* strains display elevated frequencies of post-meiotic segregation at *THR1*, although the increase is statistically significant (using Fishers Exact) only in the *zip1[Δ21-163] spo11-179* strain. The minimal and maximal values defining 95% confidence intervals for each proportion are indicated by grey bars; *the maximal values for *zip1[Δ21-163]* carrying *SPO11+*, *spo11-179* and *spo11-32* alleles are 26%, 47%, 36%, respectively. *P* values from one-way ANOVA analysis of variance, followed by the Dunnett's test for multi-comparisons of every mean to the wild type control, are as follows (left to right, beginning with *zip1[Δ21-163]*):, *P*=0.030, 0.300, 0.095, 0.750. See Table 4 for additional detail regarding the frequency of gene conversion at *THR1* and characteristic features of post-meiotic segregation events in these strains.

Figure S7

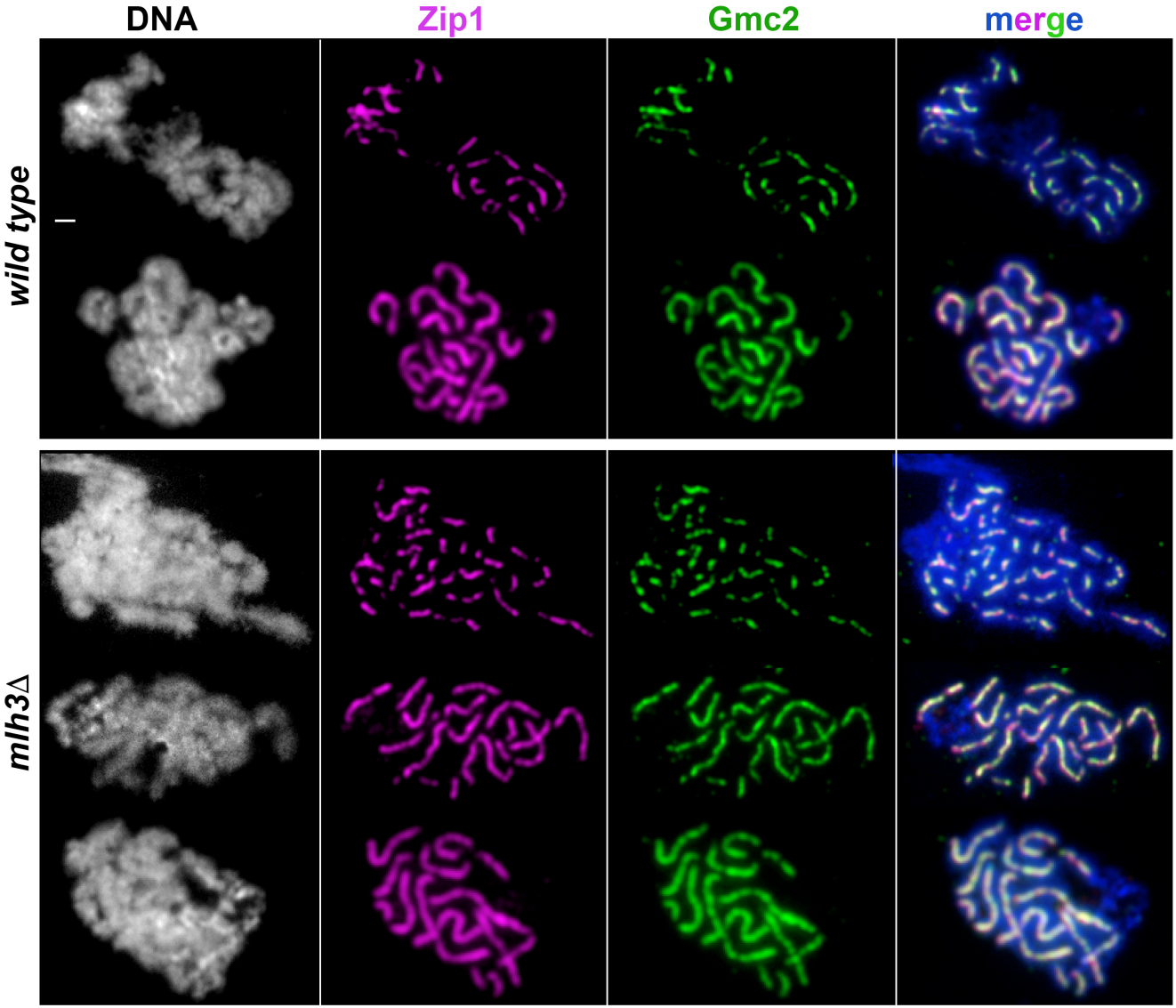
DNA
Zip1
Gmc2
merge
wild type
mlh3Δ

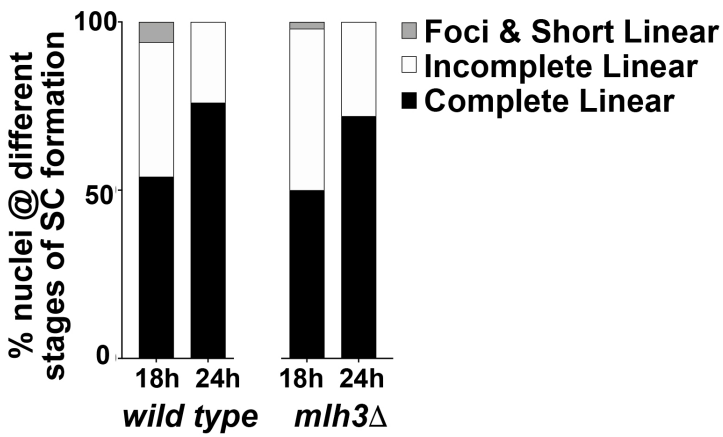
% nuclei @ different stages of SC formation
100
50
0
18h
24h
18h
24h
wild type
mlh3Δ
Foci & Short Linear
Incomplete Linear
Complete Linear

Figure S7. SC assembles with normal timing in *mlh3* mutant meiocytes.
Images show examples of surface spread mid-meiotic prophase nuclei from *MLH3* (top two rows) and *mlh3* mutant (bottom three rows) strains. Both strains are missing the transcription factor Ndt80, to ensure that all sporulating cells, which progress through meiosis at variable rates in this strain background, halt progression at late prophase with maximal SC length. For each genotype, structures consisting of coincident Zip1 (magenta) and Gmc2 (green) were evaluated in 50 nuclei at 18 and 24 hours after placement in sporulation media. As indicated in the stacked bar graph, wild-type and *mlh3* strains at both time points displayed similar proportions of nuclei with complete SC (dark shading, second, fourth and fifth row of example images), intermediate SC (white shading, top and third row of example images) or only SC protein foci on chromatin (grey shading). Scale bar, 1 μm.

Figure S8

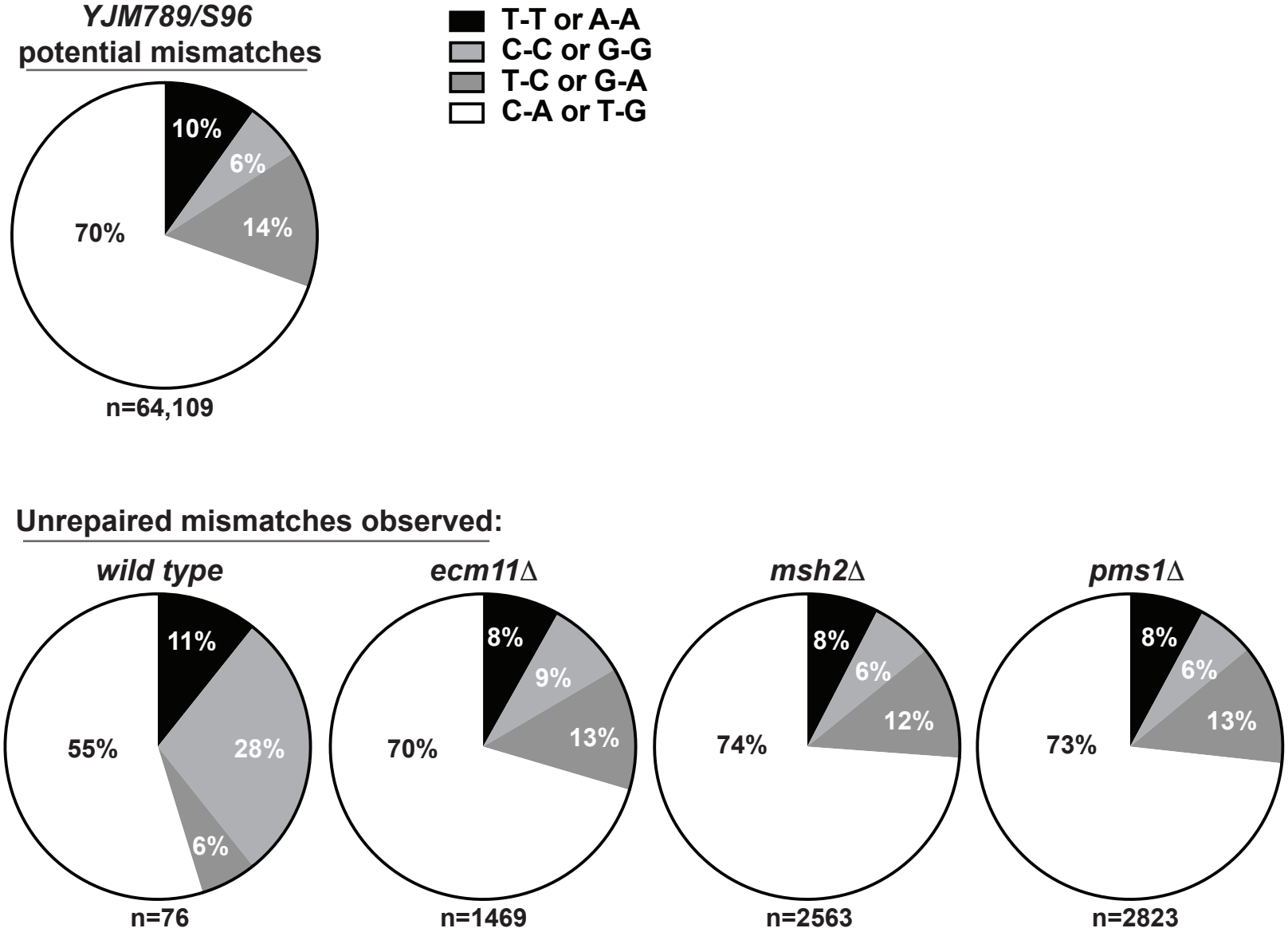
YJM789/S96
potential mismatches
T-T or A-A
C-C or G-G
T-C or G-A
C-A or T-G
10%
6%
14%
70%
n=64,109
Unrepaired mismatches observed:
wild type
11%
28%
6%
55%
n=76
ecm11Δ
8%
9%
13%
70%
n=1469
msh2Δ
8%
6%
12%
74%
n=2563
pms1Δ
8%
6%
13%
73%
n=2823

Figure S8. All mismatch types appear equally susceptible to repair failure in *ecm11*, *msh2* and *pms1* meioses.
Pie graphs display the proportion of distinct types of mismatches within each population. The upper graph gives the proportion of every potential meiotic heteroduplex mismatch type, based on the 64,109 SNPs present between the YJM789 and S96 genomic sequences. The lower graphs display the proportion of each mismatch type among PMS events (unrepaired mismatches) in four wild-type, five *ecm11*, two *msh2* and three *pms1* octad Rec-Seq datasets. Data from individual octads within each genotype are summed. Mismatch types were identified using the YJM and S96 nucleotide sequence at the coordinate of each unrepaired mismatch. If the DNA sequence coordinate in "mom" within an octad bears a "T" (the YJM nucleotide), whereas its cognate "daughter" instead bears an "A" (the S96 nucleotide), the meiotic heteroduplex is inferred to have carried an A-A or a T-T mismatch. Classes include A-A/T-T (black), C-C/G-G (light grey), T-C/G-A (dark grey), and C-A/T-G (white). Percentages are indicated over corresponding shaded components of the graphs, and below the graph is indicated the total number of mismatches classified (n) for each genotype. Note chromosome 7 recombination events for two wild-type octads were excluded from these analyses due to chromosome 7 disomy.

Table S1. Genetic map distances of strains analyzed for post-meiotic segregation at *THR1*

GENOTYPE (STRAIN)	INTERVAL (CHROMOSOME)	PD	TT	NPD	TOTAL	cM (± SE)	%WT	cM by chrm	%WT by chrm	viability
WT	*HIS4-CEN3* (III)	584	528	10	1122	**26.2 (1.1)**	**100**	103.7 (III)	**100**	
(K842)	*CEN3-MAT* (III)	708	416	4	1128	**19.5 (0.9)**	**100**			**97%**
*	*MAT-RAD18* (III)	412	676	18	1106	**35.4 (1.3)**	**100**			
	RAD18-HMR (III)	651	454	8	1113	**22.6 (1.0)**	**100**			
	SPO11-SPO13 (VIII)	453	630	33	1116	**37.1 (1.6)**	**100**	75.2 (VIII)	**100**	
	SPO13-THR1 (VIII)	913	180	2	1095	**8.8 (0.7)**	**100**			
	THR1-LYS2 (VIII)	490	590	8	1088	**29.3 (1.0)**	**100**			
ecm11Δ	*HIS4-CEN3* (III)	464	375	5	844	**24.0 (1.1)**	**92**	134.2 (III)	**129**	
(K857)	*CEN3-MAT* (III)	416	431	13	860	**29.6 (1.4)**	**152**			**92%**
*	*MAT-RAD18* (III)	263	495	29	787	**42.5 (2.0)**	**120**			
	RAD18-HMR (III)	315	457	25	797	**38.1 (1.9)**	**169**			
	SPO11-SPO13 (VIII)	342	446	40	828	**41.4 (2.2)**	**112**	115.8 (VIII)	**154**	
	SPO13-THR1 (VIII)	480	272	8	760	**21.1 (1.4)**	**240**			
	THR1-LYS2 (VIII)	216	469	53	738	**53.3 (2.7)**	**182**			
ecm11[K5R,K101R]	*HIS4-CEN3* (III)	181	229	5	415	**31.2 (1.9)**	**119**	160.5 (III)	**155**	
(K1123/K1124)	*CEN3-MAT* (III)	175	227	11	413	**35.5 (2.5)**	**182**			**93%**
	MAT-RAD18 (III)	105	259	27	391	**53.8 (3.6)**	**152**			
	RAD18-HMR (III)	157	240	15	412	**40.0 (2.8)**	**177**			
	SPO11-SPO13 (VIII)	117	275	30	422	**53.9 3.5)**	**145**	130.7 (VIII)	**174**	
	SPO13-THR1 (VIII)	243	134	3	380	**20.0 (1.8)**	**227**			
	THR1-LYS2 (VIII)	95	242	29	366	**56.8 (3.9)**	**194**			
gmc2Δ	*HIS4-CEN3* (III)	224	237	7	468	**29.8 (1.9)**	**114**	154.4 (III)	**149**	
(K906)	*CEN3-MAT* (III)	212	247	9	468	**32.2 (2.1)**	**165**			**92%**
*	*MAT-RAD18* (III)	139	280	23	442	**47.3 (3.0)**	**134**			
	RAD18-HMR (III)	119	311	15	445	**45.1 (2.5)**	**200**			
	SPO11-SPO13 (VIII)	188	251	19	458	**39.9 (2.8)**	**108**	120.3 (VIII)	**160**	
	SPO13-THR1 (VIII)	239	180	7	426	**26.1 (2.1)**	**297**			
	THR1-LYS2 (VIII)	103	277	28	408	**54.3 (3.5)**	**185**			
zip1[Δ21-163]	*HIS4-CEN3* (III)	263	311	10	584	**31.8 (1.8)**	**121**	139.9 (III)	**135**	
(AF6)	*CEN3-MAT* (III)	242	331	13	586	**34.9 (1.9)**	**179**			**89%**
**	*MAT-RAD18* (III)	208	329	17	554	**38.9 (2.2)**	**110**			
	RAD18-HMR (III)	231	320	11	562	**34.3 (1.9)**	**152**			
	SPO11-SPO13 (VIII)	182	332	44	558	**53.4 (3.2)**	**144**	124.5 (VIII)	**166**	
	SPO13-THR1 (VIII)	325	194	3	522	**20.3 (1.4)**	**231**			
	THR1-LYS2 (VIII)	162	329	34	525	**50.8 (3.0)**	**173**			
ecm11Δ zip1[Δ21-163]	*HIS4-CEN3* (III)	230	252	11	493	**32.3 (2.1)**	**123**	143.1 (III)	**138**	
(AF5)	*CEN3-MAT* (III)	186	306	11	503	**37.0 (2.1)**	**190**			**93%**
	MAT-RAD18 (III)	187	274	14	475	**37.7 (2.4)**	**106**			
	RAD18-HMR (III)	193	272	12	477	**36.1 (2.2)**	**160**			
	SPO11-SPO13 (VIII)	144	308	30	482	**50.6 (3.1)**	**136**	120.9 (VIII)	**161**	
	SPO13-THR1 (VIII)	276	177	2	455	**20.8 (1.4)**	**236**			
	THR1-LYS2 (VIII)	145	280	28	453	**49.5 (3.2)**	**169**			
msh2Δ	*HIS4-CEN3* (III)	62	77	3	142	**33.5 (3.9)**	**128**	118.6 (III)	**114**	
(AM4003)	*CEN3-MAT* (III)	98	43	1	142	**17.3 (2.8)**	**89**			**78%**
	MAT-RAD18 (III)	36	97	4	137	**44.2 (4.2)**	**125**			
	RAD18-HMR (III)	85	55	2	142	**23.6 (3.4)**	**104**			
	SPO11-SPO13 (VIII)	59	82	4	145	**36.6 (4.2)**	**99**	73.5 (VIII)	**98**	
	SPO13-THR1 (VIII)	120	22	0	142	**7.8 (1.5)**	**88**			
	THR1-LYS2 (VIII)	64	77	1	142	**29.2 (2.8)**	**100**			
pms1Δ	*HIS4-CEN3* (III)	14	7	0	21	**16.7 (5.1)**	**64**	107.6 (III)	**104**	
(AM4004)	*CEN3-MAT* (III)	12	10	0	22	**22.7 (5.3)**	**116**			**76%**
	MAT-RAD18 (III)	9	11	2	22	**52.3 (17.5)**	**148**			
	RAD18-HMR (III)	15	7	0	22	**15.9 (5.0)**	**70**			
	SPO11-SPO13 (VIII)	5	14	1	20	**50.0 (13.7)**	**135**	85.2 (VIII)	**113**	
	SPO13-THR1 (VIII)	17	5	0	22	**11.4 (4.5)**	**130**			
	THR1-LYS2 (VIII)	11	10	0	21	**23.8 (5.5)**	**81**			
zip1[Δ21-163] SPO11+	*HIS4-CEN3 (III)*	186	207	9	402	**32.5 (2.4)**	**124**	134.2 (III)	**129**	
(K1765)	*CEN3-MAT (III)*	156	243	6	405	**34.4 (2.0)**	**176**			**92%**
(CRISPR *SPO11* allele)	*MAT-RAD18 (III)*	160	213	13	386	**37.7 (2.8)**	**106**			
	RAD18-HMR (III)	195	191	7	393	**29.6 (2.2)**	**130**			
	SPO13-THR1 (VIII)	233	142	2	377	**20.4 (1.6)**	**232**	60.6 (VIII)	**159**	
	THR1-LYS2 (VIII)	124	244	10	378	**40.2 (2.5)**	**137**			
zip1[Δ21-163] spo11-179	*HIS4-CEN3 (III)*	460	167	0	627	**13.3 (0.9)**	**51**	73.7 (III)	**71**	
(K1830)	*CEN3-MAT (III)*	426	205	2	633	**17.1 (1.1)**	**87**			**82%**
(CRISPR *spo11* allele)	*MAT-RAD18 (III)*	288	334	6	628	**29.5 (1.5)**	**83**			
	RAD18-HMR (III)	465	162	2	629	**13.8 (1.1)**	**61**			
	SPO13-THR1 (VIII)	523	94	0	617	**7.6 (0.7)**	**86**	50.0 (VIII)	**131**	
	THR1-LYS2 (VIII)	189	407	19	615	**42.4 (2.1)**	**144**			
zip1[Δ21-163] spo11-32	*HIS4-CEN3 (III)*	821	188	6	1015	**11.0 (0.9)**	**42**	64.2 (III)	**62**	
(K1767)	*CEN3-MAT (III)*	814	185	9	1008	**11.9 (1.1)**	**61**			**65%**
(CRISPR *spo11* allele)	*MAT-RAD18 (III)*	448	539	10	997	**30.0 (1.2)**	**85**			
	RAD18-HMR (III)	824	173	9	1006	**11.3 (1.1)**	**50**			
	SPO13-THR1 (VIII)	906	97	0	1003	**4.8 (0.5)**	**55**	36.9 (VIII)	**97**	
	THR1-LYS2 (VIII)	429	558	14	1001	**32.1 (1.3)**	**109**			

GENOTYPE (STRAIN)	INTERVAL (CHROMOSOME)	PD	TT	NPD	TOTAL	cM (± SE)	%WT	cM by chrm	%WT by chrm	viability
zip3Δ	*HIS4-CEN3* (III)	323	161	10	494	**22.4 (2.1)**	**85**	87.1 (III)	**84**	
(K926)	*CEN3-MAT* (III)	328	167	5	500	**19.7 (1.6)**	**101**			**81%**
**	*MAT-RAD18* (III)	319	154	10	483	**22.2 (2.1)**	**63**			
	RAD18-HMR (III)	306	174	8	488	**22.8 (2.0)**	**101**			
	SPO11-SPO13 (VIII)	336	120	7	463	**17.5 (1.9)**	**47**	35.8 (VIII)	**48**	
	SPO13-THR1 (VIII)	429	44	1	474	**5.3 (0.9)**	**60**			
	THR1-LYS2 (VIII)	369	98	4	471	**13.0 (1.5)**	**44**			
msh4Δ	*HIS4-CEN3* (III)	375	96	1	472	**10.8 (1.1)**	**41**	53.4 (III)	**51**	
(K852)	*CEN3-MAT* (III)	425	51	1	477	**6.0 (0.9)**	**31**			**71%**
*	*MAT-RAD18* (III)	276	184	7	467	**24.2 (1.9)**	**68**			
	RAD18-HMR (III)	352	116	0	468	**12.4 (1.0)**	**55**			
	SPO11-SPO13 (VIII)	365	89	3	457	**11.7 (1.4)**	**32**	30.4 (VIII)	**40**	
	SPO13-THR1 (VIII)	423	27	0	450	**3.0 (0.6)**	**34**			
	THR1-LYS2 (VIII)	319	129	2	450	**15.7 (1.4)**	**54**			
zip3Δ msh4Δ	*HIS4-CEN3* (III)	353	194	10	557	**22.8 (1.9)**	**87**	92.3 (III)	**89**	
(AM3658/AM3659)	*CEN3-MAT* (III)	368	193	8	569	**21.2 (1.7)**	**109**			**79%**
**	*MAT-RAD18* (III)	344	177	11	532	**22.8 (2.0)**	**64**			
	RAD18-HMR (III)	330	210	12	552	**25.5 (2.0)**	**113**			
	SPO11-SPO13 (VIII)	360	179	8	547	**20.8 (1.8)**	**56**	42.5 (VIII)	**57**	
	SPO13-THR1 (VIII)	464	64	1	529	**6.6 (0.9)**	**75**			
	THR1-LYS2 (VIII)	392	129	5	526	**15.1 (1.5)**	**52**			
ecm11Δ msh4Δ	*HIS4-CEN3* (III)	358	51	0	409	**6.2 (0.8)**	**24**	49.6 (III)	**48**	
(K882)	*CEN3-MAT* (III)	383	28	1	412	**4.1 (1.0)**	**21**			**58%**
*	*MAT-RAD18* (III)	237	153	5	395	**23.2 (2.0)**	**66**			
	RAD18-HMR (III)	292	105	4	401	**16.1 (1.8)**	**71**			
	SPO11-SPO13 (VIII)	339	56	0	395	**7.1 (0.9)**	**19**	36.5 (VIII)	**49**	
	SPO13-THR1 (VIII)	341	35	0	376	**4.7 (0.8)**	**53**			
	THR1-LYS2 (VIII)	244	118	11	373	**24.7 (2.8)**	**84**			
mlh3Δ	*HIS4-CEN3* (III)	663	285	2	950	**15.6 (0.9)**	**60**	63.1 (III)	**61**	
(K854)	*CEN3-MAT* (III)	764	185	3	952	**10.7 (0.8)**	**55**			**86%**
*	*MAT-RAD18* (III)	526	398	11	935	**24.8 (1.3)**	**70**			
	RAD18-HMR (III)	725	213	2	940	**12.0 (0.8)**	**53**			
	SPO11-SPO13 (VIII)	604	330	10	944	**20.7 (1.2)**	**32**	31.4 (VIII)	**42**	
	SPO13-THR1 (VIII)	871	67	0	938	**3.6 (0.4)**	**41**			
	THR1-LYS2 (VIII)	648	282	2	932	**15.8 (0.9)**	**54**			
mlh3Δ zip3Δ	*HIS4-CEN3* (III)	156	44	2	202	**13.9 (2.5)**	**53**	74.4 (III)	**72**	
(K1046)	*CEN3-MAT* (III)	145	63	4	212	**20.5 (3.1)**	**105**			**74%**
	MAT-RAD18 (III)	135	60	2	197	**18.3 (2.6)**	**52**			
	RAD18-HMR (III)	121	74	2	197	**21.7 (2.7)**	**96**			
	SPO11-SPO13 (VIII)	143	55	1	199	**15.3 (2.1)**	**41**	40.8 (VIII)	**54**	
	SPO13-THR1 (VIII)	172	19	0	191	**5.0 (1.1)**	**57**			
	THR1-LYS2 (VIII)	126	59	3	188	**20.5 (3.1)**	**70**			
mlh3Δ msh4Δ	*HIS4-CEN3* (III)	292	51	1	344	**8.3 (1.3)**	**32**	52.8 (III)	**51**	
(K1049)	*CEN3-MAT* (III)	308	44	0	352	**6.3 (0.9)**	**32**			**54%**
	MAT-RAD18 (III)	211	128	4	343	**22.2 (2.1)**	**63**			
	RAD18-HMR (III)	234	110	0	344	**16.0 (1.3)**	**71**			
	SPO11-SPO13 (VIII)	243	90	2	335	**15.2 (1.7)**	**41**	37.5 (VIII)	**50**	
	SPO13-THR1 (VIII)	291	25	1	317	**4.9 (1.2)**	**56**			
	THR1-LYS2 (VIII)	231	80	5	316	**17.4 (2.4)**	**59**			
ecm11Δ mlh3Δ	*HIS4-CEN3* (III)	836	296	10	1142	**15.6 (1.0)**	**60**	87.9 (III)	**85**	
(AM3896/ AM3897/K888)	*CEN3-MAT* (III)	839	302	8	1149	**15.2 (1.0)**	**78**			**89%**
*	*MAT-RAD18* (III)	527	464	34	1025	**32.6 (1.7)**	**92**			
	RAD18-HMR (III)	635	381	21	1037	**24.5 (1.4)**	**108**			
	SPO11-SPO13 (VIII)	689	401	22	1112	**24.0 (1.4)**	**65**	75.7 (VIII)	**101**	
	SPO13-THR1 (VIII)	794	213	8	1015	**12.9 (1.0)**	**147**			
	THR1-LYS2 (VIII)	439	473	45	957	**38.8 (2.0)**	**132**			
K. lactis ZIP1	*HIS4-CEN3* (III)	285	207	13	505	**28.2 (2.3)**	**108**	101.5 (III)	**98**	
(AS1)	*CEN3-MAT* (III)	308	211	9	528	**25.1 (1.9)**	**129**			**77%**
	MAT-RAD18 (III)	310	181	12	503	**25.1 (2.2)**	**71**			
	RAD18-HMR (III)	316	188	8	512	**23.1 (1.9)**	**102**			
	SPO11-SPO13 (VIII)	281	196	25	502	**34.5 (2.9)**	**93**	66.0 (VIII)	**88**	
	SPO13-THR1 (VIII)	374	99	0	473	**10.5 (0.9)**	**119**			
	THR1-LYS2 (VIII)	310	157	7	474	**21.0 (1.9)**	**72**			
mlh3Δ K. lactis ZIP1	*HIS4-CEN3* (III)	317	208	13	538	**26.6 (2.1)**	**102**	99.0 (III)	**95**	
(AS19)	*CEN3-MAT* (III)	320	220	10	550	**25.5 (1.9)**	**131**			**72%**
	MAT-RAD18 (III)	321	200	8	529	**23.4 (1.8)**	**66**			
	RAD18-HMR (III)	327	195	9	531	**23.5 (1.9)**	**104**			
	SPO11-SPO13 (VIII)	289	212	20	521	**31.9 (2.6)**	**86**	59.7 (VIII)	**79**	
	SPO13-THR1 (VIII)	412	85	0	497	**8.6 (0.8)**	**98**			
	THR1-LYS2 (VIII)	352	137	9	498	**19.2 (2.0)**	**66**			

At least some data for strains marked * or ** were previously published in (VOELKEL-MEIMAN et al. 2016)*, or (VOELKEL-MEIMAN et al. 2019)**

Table S1. Genetic map distances of strains analyzed for post-meiotic segregation at *THR1*.
(Relates to Figures 1, 7, S6)
Map distances were calculated using tetrad analysis as described previously (VOELKEL-MEIMAN *et al*. 2019) in strains heterozygous for the following nine alleles: *his4-260,519, hphMX@CEN3, MAT*a, *ADE2@RAD18, natMX@HMR* (on chromosome *III*); *TRP1+@SPO11, spo13::URA3+, thr1-4*, *LYS2@210kb* (on chromosome VIII). Four spore-viable tetrads with no more than seven gene conversion (non-2:2) events were included in calculations. See Tables 1 and 4 for *THR1* gene conversion and post-meiotic segregation frequencies. Table indicates map distances and their corresponding percentages of the wild-type values for individual intervals, and the corresponding percentage of wild-type cumulative chromosomal map distance for chromosome III and VIII. Some data from this table is plotted in Figure S6. At least some of the data for strains marked * or ** were previously published in (VOELKEL-MEIMAN *et al*. 2016)*, or (VOELKEL-MEIMAN *et al*. 2019)**.

Table S2. The frequency of unrepaired mismatches among recombination events with different gene conversion tract lengths

A	**%** of **noncrossover** GC tracts of different lengths (n) that carry an unrepaired mismatch						
	0-1000 bp	1001-2000bp	2001-3000bp	3001-4000bp	4001-10,000bp	10,001-20,000bp	20,000+bp
wt	15.4 (26)	4.6 (44)	16.0 (25)	5.0 (20)	23.1 (13)	n/a (0)	n/a (0)
ecm11	**30.2 (96)**	**15.6 (109)**	**22.9 (70)**	**30.0 (40)**	**44.9 (98)**	**20.0 (10)**	**0 (1)**
msh2	95.5 (66)	97.8 (45)	100.0 (17)	100.0 (7)	61.5 (13)	n/a (0)	n/a (0)
pms1	78.4 (125)	81.1 (74)	87.5 (40)	94.7 (19)	47.1 (17)	100.0 (1)	n/a (0)

B	**%** of **crossover** GC tracts of different lengths (n) that carry an unrepaired mismatch						
	0-1000 bp	1001-2000bp	2001-3000bp	3001-4000bp	4001-10,000bp	10,001-20,000bp	20,000+bp
wt	5.2 (136)	12.0 (83)	17.9 (56)	13.7 (51)	13.6 (59)	25.0 (4)	n/a (0)
ecm11	**24.7 (186)**	**37.5 (104)**	**51.1 (88)**	**54.7 (106)**	**63.5 (342)**	**86.9 (46)**	**0 (2)**
msh2	36.1 (97)	91.9 (99)	91.1 (45)	100.0 (30)	100.0 (38)	n/a (0)	n/a (0)
pms1	42.2 (121)	82.8 (87)	78.3 (60)	81.4 (43)	75.8 (33)	100.0 (1)	0 (1)

Table S2. Frequency of unrepaired mismatches among recombination events with different gene conversion tract lengths.

(Relates to Figure S4)

The percentage of unrepaired mismatch-carrying noncrossover (**A**) or crossover (**B**) events with specific gene conversion tract lengths. Data is consolidated from all genome-wide recombination events identified in four wild-type, five *ecm11*, two *msh2* and three *pms1* meioses (Octad Rec-Seq datasets). For each category of gene conversion tract lengths, a Fisher's Exact test was used to determine whether the proportion of mismatch-carrying recombination events is significantly different in any of the mutant strains relative to wild-type (*P* values are indicated on the Figure S4 graphs; red indicates statistical significance).

Table S3. The per-nucleotide frequency of unrepaired mismatches in wild-type, *ecm11*, *msh2*, and *pms1* meioses

A **NONCROSSOVER EVENTS**

	Unrepaired mismatch - containing GC tract length (cumulative bp)	Total unrepaired mismatches among all events	Unrepaired mismatches per bp of GC tract, for **mismatch-carrying events**	Fishers Exact, two sided *P*	**Mismatch-free** GC tract length (cumulative bp)	Unrepaired mismatches per bp of GC tract, for **all events**	Chi square with Yates Correction, two sided *P*
wild type	35309	17	4.81E-04		243858	6.09E-05	
ecm11	416823	255	6.12E-04	0.428	844793	2.02E-04	**<0.0001**
msh2	207732	802	3.86E-03	**<0.0001**	30807	3.36E-03	**<0.0001**
pms1	345315	1194	3.46E-03	**<0.0001**	99791	2.68E-03	**<0.0001**

B **CROSSOVER EVENTS**

	Unrepaired mismatch - containing GC tract length (cumulative bp)	Total unrepaired mismatches among all events	Unrepaired mismatches per bp of GC tract, for **mismatch-carrying events**	Chi square with Yates Correction, two sided *P*	**Mismatch-free** GC tract length (cumulative bp)	Unrepaired mismatches per bp of GC tract, for **all events**	Chi square with Yates Correction, two sided *P*
wild type	127351	59	4.63E-04		789499	6.44E-05	
ecm11	2270528	1214	5.35E-04	0.311	1322763	3.38E-04	**<0.0001**
msh2	494207	1761	3.56E-03	**<0.0001**	37193	3.31E-03	**<0.0001**
pms1	605311	1629	2.69E-03	**<0.0001**	145097	2.17E-03	**<0.0001**

Table S3. Per-nucleotide frequency of unrepaired mismatches in wild-type, *ecm11*, *msh2*, and *pms1* meioses.

(Relates to Figure 5)

Table lists the per-nucleotide frequency of unrepaired mismatches identified among the sum total of noncrossover (**A**) and crossover (**B**) recombination events in four wild type, five *ecm11*, two *msh2*, and three *pms1* Octad Rec-Seq datasets. In the columns to the left of the vertical midline, an unrepaired mismatch per-nucleotide frequency *exclusive to mismatch-carrying events* was calculated by dividing the total number of unrepaired mismatches found in a given genotype by the cumulative gene conversion tract length of events carrying an unrepaired mismatch in that strain. In columns on the right of the midline, the mismatch per nucleotide frequency for *all events* was calculated by dividing the total number of unrepaired mismatches by the cumulative gene conversion tract length of all events. Chi square with Yates Correction analysis found that defective mismatch repair events are significantly more frequent among both noncrossover and crossover events in *ecm11* relative to wild-type. However, among those select recombination events susceptible to inefficient mismatch repair, the unrepaired mismatch frequency is not significantly different between *ecm11* and wild-type (according to a Fisher's Exact test or Chi square with Yates Correction). See Figure 5 legend for additional statistical analysis. Note chromosome 7 recombination events for two wild-type octads were excluded from these analyses, due to chromosome 7 disomy.

Table S4. Strains used in this study

	GENOTYPE
YAM1252	*lys2ΔNhe his4-260,519 leu2-3,112 MATα trp1-289 ura3-1 thr1-4 ade2-1* *lys2ΔNhe his4-260,519 leu2-3,112 MAT**a** trp1-289 ura3-1 thr1-4 ade2-1*
K842	*lys2ΔNhe HIS4 leu2-3,112 hphMX4@CEN3 MATα ADE2@RAD18 natMX4@HMR* *lys2ΔNhe his4-260,519 leu2-3,112 CEN3 MAT**a** RAD18 HMR* *trp1-289 ura3-1 TRP1MX4@SPO11 spo13::URA3 THR1 210kb ade2-1* *trp1-289 ura3-1 SPO11 SPO13 thr1-4 LYS2@210kb ade2-1*
K857	K842 homozygous *ecm11::LEU2*
K1123/ K1124	K842 homozygous *ecm11[K5R, K101R]*
K906	K842 homozygous *gmc2::kanMX4*
AF6	K842 homozygous *zip1[Δ21-163]*
AF5	AF6 *ecm11::kanMX4*
AM4003	K842 homozygous *msh2::kanMX4*
AM3697	*lys2ΔNhe HIS4 leu2-3,112 hphMX4@CEN3 MATα ADE2@RAD18 natMX4@HMR* *LYS2 his4-260,519 leu2-3,112 CEN3 MAT**a** RAD18 HMR* *trp1-289 URA3 TRP1MX4@SPO11 THR1 210kb msh2::kanMX4 ade2-1* *trp1-289 ura3-1 SPO11 thr1-4 LYS2@210kb msh2::kanMX4 ade2-1*
AM3696	AM3697 homozygous *MSH2 pms1::kanMX4 natMX4@HMR*
AM4004	K842 homozygous *pms1::kanMX4*
Octad Rec-Seq experiments	
AM3740	***YJM789*** *(YEM045 isolate) MATα ho::his6 AMN1[A1103T]* ***YJMS96*** *MAT**a** ho::his6 AMN1*
AM3735	AM3740 homozygous *ecm11::kanMX4*
AM3736	AM3740 homozygous *msh2::hphMX4*
AM3738	AM3740 homozygous *pms1::hphMX4*
K926	K842 homozygous *zip3::kanMX4*
K852	K842 homozygous *msh4::kanMX4*
AM3658/ AM3659	K842 homozygous *zip3::kanMX4 msh4::LEU2*
K882	K857 homozygous *msh4::kanMX4*
K854	K842 homozygous *mlh3::kanMX4*
K1046	K842 homozygous *mlh3::LEU2 zip3::kanMX4*
K1049	K842 homozygous *mlh3::LEU2 msh4::kanMX4*
AM3896/ AM3897/ K888	K857 homozygous *mlh3::kanMX4*

AS1	K842 homozygous *K. lactis ZIP1*
AS19	AS1 homozygous *mlh3::kanMX4*
K1765	AF6 homozygous *SPO11* (*SPO11* inserted by CRISPR cas9 *spo11::kanMX4* haploid parent strains)
K1830	AF6 homozygous *spo11-179 (spo11-N137K, K317I, T365S)* (*spo11-179* inserted by CRISPR cas9 *spo11::kanMX4* haploid parent strains)
K1767	AF6 homozygous *spo11-32 (spo11-L254H)* (*spo11-32* inserted by CRISPR cas9 *spo11::kanMX4* haploid parent strains)
AM5083	YAM1252 homozygous *ndt80::LEU2*
AM5086	AM5083 homozygous *mlh3::hphMX*

Table S4. Strains used in this study.

Strains are of the BR1919-8B background (ROCKMILL AND ROEDER 1998), except for those listed under the heading "Octad Rec Seq Experiments", which are derived from a cross between YJM789 and S96 genetic backgrounds (WEI *et al*. 2007; ANDERSON *et al*. 2011).

Table S5. Spore viabilities of hybrid strains.

Genotype (strain)	Tetrads dissected	4 spore viable	3 spore viable	2 spore viable	1 spore viable	0 spore viable	Spore viability (%)
wild type (AM3740)	66	40	15	6	3	2	83
ecm11 (AM3735)	155	34	60	36	18	7	65
msh2 (AM3736)	102	16	16	30	29	11	49
pms1 (AM3738)	92	17	18	28	21	8	54